Theoret. chim. Acta (Berl.) 19, 109—120 (1970)

Commentationes

Influence of Long-Range Coulombic Interactions on Binding Energy Curves of Molecule-Ions*

M. J. FEINBERG

Department of Chemistry, Tufts University Medford, Massachusetts 02155, USA

Received June 8, 1970

Potential barriers occur on binding energy curves of certain diatomic molecule-ions. The origin of such barriers is discussed for the prototype case consisting of a single electron moving in the field of two nuclei with equal but arbitrary charges. A procedure for determining stationary points on the binding energy curves is developed and applied to the lowest Σ_g and Σ_u states. The binding energy is expressed as a sum of promotional, coulombic and resonance contributions, and these components are studied as functions of the internuclear distance. The analysis demonstrates that the energy maxima on the Σ_g curves arise from long-range coulombic repulsions, and are unrelated to centrifugal potentials of nuclear motion and the mechanisms of predissociation. In addition, the analysis shows that long-range attractions can occur and introduce binding character into normally antibinding states.

In den Bindungsenergie-Kurven gewisser zweiatomiger Molekül-Ionen treten Potential-Schwellen auf. Der Ursprung solcher Barrieren wird für den Prototyp diskutiert, der aus einem einzigen Elektron im Feld zweier Kerne mit beliebigen, gleichen Ladungen besteht.

Ein Verfahren zur Bestimmung stationärer Punkte auf den Bindungsenergie-Kurven wird entwickelt und auf die niedrigsten Σ_g- und Σ_u-Zustände angewendet. Die Bindungsenergie wird als eine Summe von Promotions-, Coulomb- und Resonanz-Anteilen dargestellt; der Verlauf dieser Anteile in Abhängigkeit vom Kernabstand wird untersucht. Die Analyse zeigt, daß die Energiemaxima auf Σ_g-Kurven von der Coulombabstoßung für große Abstände herrühren, und daß sie nicht in Beziehung zu Zentrifugalpotentialen der Kernbewegung und dem Mechanismus der Prädissoziation stehen. Weiterhin zeigt die Untersuchung, daß auch Anziehung für große Abstände auftreten kann, die den normalerweise antibindenden Zuständen bindenden Charakter verleiht.

Des barrières de potentiel apparaissent sur les courbes d'énergie de liaison de certains ions de molécules diatomiques. L'origine de ces barrières est discutée pour le cas prototype d'un électron unique se déplaçant dans le champ de deux noyaux de charges arbitraires égales. Un procédé pour déterminer les points stationnaires des courbes d'énergie de liaison est développé et appliqué aux plus bas états Σ_g et Σ_u. L'énergie de liaison est exprimée comme somme de contributions de type promotion, coulombien et résonance; ces composantes sont étudiées en fonction de la distance internucléaire. Cette analyse démontre que les maxima d'énergie sur les courbes Σ_g proviennent des répulsions coulombiennes à longue distance et ne sont pas liés aux potentiels centrifuges du mouvement nucléaire ou aux mécanismes de prédissociation. De plus, l'analyse montre que des attractions à longue distance peuvent se produire et introduire un caractère liant dans des états normalement antiliants.

1. Introduction

It has been known for some time that potential barriers occur in binding energy curves of certain diatomic ions. Such barriers were obtained, in particular, from the theoretical calculations for He_2^{++} by Pauling [1] and more

* Contribution No. 386 from the Department of Chemistry, Tufts University. Work done in part at the Ames Laboratory of the U.S. Atomic Energy Commission, Iowa State University, Ames, Iowa 50010. Contribution No. 2589.

recently by Fraga and Ransil [2]. The general homonuclear, two-electron system with arbitrary nuclear charges was investigated by Feinberg and Haas [3] who showed that such barriers arise for any value of the nuclear charge different from unity. Cohen and McEachran [4] recently reported related results for systems consisting of one-electron in the field of two nuclei with identical but arbitrary charges.

In neutral systems potential barriers are known to arise for two reasons: the centrifugal potential of nuclear motion and the crossing of energy curves of different electronic states. While, occasionally, some authors have thought that these two mechanisms could also be relevant for the barriers found in the ionic systems mentioned, Pauling [1] has suggested an electrostatic explanation instead.

Recently a new type of analysis for the origin of chemical binding has been developed and applied to H_2^+ [5, 6]. It seemed a worthwhile challenge to test the efficacy of this approach by applying it to systems exhibiting the aforementioned kind of barrier, and the present note contains the analysis of the one-electron systems discussed in Ref. [4]. The investigation shows that this *quantitative* analysis is well suited to elucidate the origin of the barriers found in these systems. It demonstrates that they are *unrelated* to centrifugal effects or curve crossings, but indeed arise from long-range coulombic repulsions in agreement with Pauling's qualitative ideas [1]. Moreover, the analysis reveals that, under appropriate conditions, analogous long-range coulombic interactions may lead to attractive effects which, in fact, can introduce binding character into states normally considered antibinding. Thus, in addition to centrifugal effects and predissociation, long-range coulombic interactions represent another, independent source for – positive or negative – "humps" on binding energy curves of molecular-ions.

2. Stationary Points on Energy Curves

In the present paper we consider the (Z, Z) molecule-ion which consists of a single electron moving in the field of two nuclei, each with charge Z and separated by distance R. Since no electron repulsion terms appear in the molecular Hamiltonian operator, it is possible to deduce all properties of these systems from numerical results for the H_2^+ molecule-ion.

2.1. Exact Wave Function

Let $E_{el}(R, Z)$ be the exact electronic energy and $E^B(R, Z)$ the binding energy[1] of the (Z, Z) molecule-ion. Thus,

$$E^B(R, Z) = E_{el}(R, Z) + \frac{Z^2}{R} + \frac{1}{2}Z^2. \tag{1}$$

[1] In the sequel, both the lowest Σ_g ("binding") and Σ_u ("antibinding") states will be discussed. In both cases, the energy difference E(molecule) – E(separated atoms) will be denoted by E^B and called the "binding energy". The reason is that positive as well as negative values of E^B will be found for both states.

This satisfies the virial theorem

$$T^B(R, Z) + E^B(R, Z) + R\left[\frac{dE^B(R, Z)}{dR}\right] = 0 \tag{2}$$

where $T^B(R, Z)$ is the kinetic energy of binding.

As mentioned by Cohen, Dorrell, and Mc Eachran [7], one has

$$E_{el}(R, Z) = Z^2 E_{el}(\bar{R}, 1) \tag{3}$$

with

$$\bar{R} = RZ\,. \tag{4}$$

Here, $E_{el}(\bar{R}, 1)$ represents the exact electronic energy of H_2^+ calculated for the distance $\bar{R}$ between the protons. From this and Eq. (1), it readily follows that

$$E^B(R, Z) = Z^2\left\{E^B(\bar{R}, 1) + \frac{Z-1}{\bar{R}}\right\}, \tag{5}$$

$$T^B(R, Z) = Z^2 T^B(\bar{R}, 1)\,, \tag{6}$$

$$V^B(R, Z) = Z^2\left\{V^B(\bar{R}, 1) + \frac{Z-1}{\bar{R}}\right\} \tag{7}$$

with V^B being the potential energy of binding.

If $E^B(R, Z)$ is stationary at $R = R_0$, the virial theorem of Eq. (2) reduces to

$$T^B(R_0, Z) + E^B(R_0, Z) = 0\,. \tag{8}$$

Substitution of Eqs. (5) and (6) into this equation yields

$$Z = 1 - \bar{R}_0\{E^B(\bar{R}_0, 1) + T^B(\bar{R}_0, 1)\} \tag{9}$$

for finite values of $\bar{R}_0$. Here,

$$\bar{R}_0 = R_0 Z \tag{10}$$

is the value of $\bar{R}$ which corresponds to the distance R_0 at which the curve $E^B(R, Z)$ is stationary. Eq. (9) in conjunction with Eq. (10) gives then an implicit relation

$$F(R_0, Z) = 0$$

which determines the point R_0 where $\partial E^B(R, Z)/\partial R$ vanishes. Thus, if the curves $E^B(\bar{R}, 1)$ and $T^B(\bar{R}, 1)$ are known for H_2^+, it is possible to calculate the stationary points R_0 for $E^B(R, Z)$ and then the corresponding energies $E^B(R_0, Z)$. If $T^B(\bar{R}, 1)$ vs. $\bar{R}$ is not available, it can be replaced by

$$T^B(\bar{R}, 1) = E^B(\bar{R}, 1) - \bar{R}\left[\frac{dE^B(\bar{R}, 1)}{d\bar{R}}\right] \tag{2'}$$

to give

$$Z = 1 - \bar{R}_0^2\left[\frac{dE^B(\bar{R}_0, 1)}{d\bar{R}_0}\right]. \tag{9'}$$

The slope of the energy for H_2^+ as a function of distance can be found by numerical differentiation of the exact energy curve.

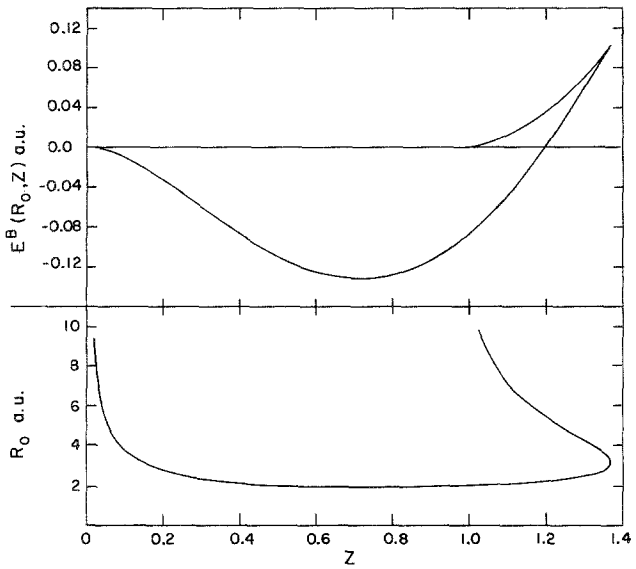

Fig. 1. Stationary points (minima and maxima), R_0, and corresponding energies, $E^B(R_0, Z)$ on the Σ_g energy curves as functions of the nuclear charge Z (Guillemin-Zener approximation)

Depending on the value of Z, one finds three cases: i) no stationary points; ii) one stationary point – at the equilibrium position; iii) two stationary points – one at the equilibrium position and the other at the maximum of a hump which appears between equilibrium and the separated atoms. A procedure for obtaining accurate information about these stationary points is as follows:

a) Rather than considering R_0 as depending upon the choice of Z, consider Z as a function of the variable $\bar{R}_0$, according to the Eq. (9). Thus enter $\bar{R}_0$ and the corresponding values of $T^B(\bar{R}_0, 1)$ and $E^B(\bar{R}_0, 1)$ into Eq. (9) to obtain Z.

b) Then obtain R_0 by substituting $\bar{R}_0$ and the corresponding Z value into Eq. (10).

c) Finally, find $E^B(R_0, Z)$ the energy at the stationary point, by substituting $\bar{R}_0 = R_0 Z$ and Z into Eq. (5).

d) The sets of values of R_0 and $E^B(R_0, Z)$ found in this way are then plotted against the corresponding Z values for a given electronic state.

If a)–d) are applied to the exact wave function for the Σ_g binding state of H_2^+, one obtains the curves shown in Fig. 1[2]. The lower curve is a plot of R_0 as a function of Z. The upper curve gives the corresponding energies, $E^B(R_0, Z)$. Thus, if a vertical line is drawn on the graph for a given value of Z, the intersections of the line with the curves yield the energies and locations of stationary points on the associated (Z, Z) energy curve.

From these results we observe that the deepest energy minimum occurs for $Z \sim 0.75$ with an energy of -0.14 a.u. at $R_0 \sim 2.0$ a.u.[3]. The exact values of Z

[2] Actually, the Guillemin-Zener function [8, 9] has been used to generate these curves. This approximation is an excellent facsimile of the exact wave function. If the latter was used, the results would be indistinguishable from those displayed in Fig. 1.

[3] The value of $Z \sim 0.5$ given in Ref. [4] is in error.

and R_0 for which this occurs may be obtained by solving the system of equations consisting of Eq. (9) and

$$\frac{\partial E^B(R_0, Z)}{\partial Z} = 0$$

or

$$Z = \tfrac{1}{2}\{1 - \bar{R}_0[E^B(\bar{R}_0, 1) - T^B(\bar{R}_0, 1)]\}.$$

Secondly, when $Z \sim 1.44$, the relative maximum and minimum coalesce to give everywhere repulsive energy curves for larger values of Z.

2.2. *Approximate Wave Functions*

It can easily be shown that Eqs. (3) and (4) apply also to approximate wave functions for H_2^+. Furthermore, if Eq. (2) is satisfied by an approximate wave function for $Z = 1.0$, then by virtue of Eqs. (4), (5), and (6), Eq. (2) is valid for arbitrary Z as well. Thus, Eq. (9) and its consequences are directly applicable to approximate results for H_2^+ if the wave function satisfies the virial theorem. This condition can always be met if the approximate function is scaled, and the scale parameter optimized by the variation method [10]. Since in this case $E^B(\bar{R}, 1)$ is variationally minimized, the corresponding values of $E^B(R, Z)$ are also minimized with respect to the scale parameter.

2.3. *Application to the Finkelstein-Horowitz Type Function*

As an application, consider the Finkelstein-Horowitz approximation to the ground and first excited state of H_2^+ [11]. This function has the form

$$\psi_\pm = [2(1 \pm S)^{-\frac{1}{2}}[A \pm B] \tag{11}$$

where A and B are 1*s* atomic orbitals. They contain orbital exponents, ζ, which are variationally determined (independently for ζ_+ and ζ_-) for each internuclear distance so that $\zeta_+ = \zeta_+(R)$ and $\zeta_- = \zeta_-(R)$. S is the overlap integral, and the "+" and "−" signs refer to the Σ_g binding state and lowest Σ_u antibinding state, respectively.

Recent variation calculations for this function have been reported elsewhere in the literature [6, 9]. If these results are used in conjunction with Eqs. (9), (10) and (5), one obtains the curves shown in Figs. 2 and 3 for the Σ_g and Σ_u states, respectively[4].

A comparison of the curves in Figs. 1 and 2 shows that the Finkelstein-Horowitz results are in excellent qualitative agreement with those obtained from the exact function. If a careful quantitative comparison is made between the energy portions of these diagrams, one finds that, as Z increases, the exact function gives increasingly lower energies. The reason for this lies in the fact that the exact function (as reproduced by the Guillemin-Zener approximation) includes orbital distortion effects which become energetically more important as Z

[4] In the Σ_u case, Eq. (9) yields negative values of Z for small and intermediate $\bar{R}_0$. These values of Z are mathematical artifacts of Eq. (9) and have no physical meaning.

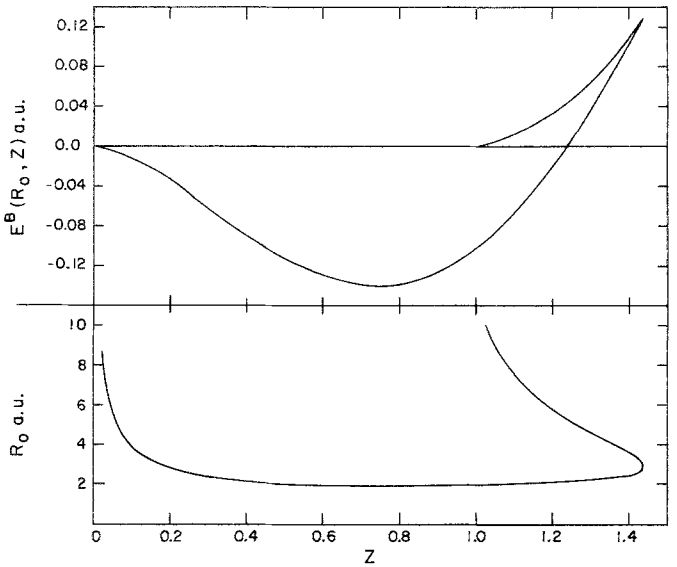

Fig. 2. Stationary points (minima and maximas), R_0, and corresponding energies, $E^B(R_0, Z)$ on Σ_g energy curves as functions of the nuclear charge Z (Finkelstein-Horowitz approximation)

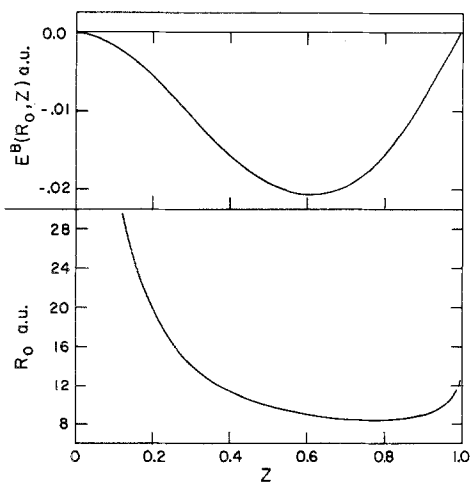

Fig. 3. Stationary points (minima), R_0, and corresponding energies, $E^B(R_0, Z)$ on Σ_u energy curves as functions of the nuclear charge Z (Finkelstein-Horowitz approximation)

increases[5]. These are small, however, and for our purposes the Finkelstein-Horowitz function serves well as basis for the energy curve analysis given in the next section.

From Fig. 2 (or Fig. 1), one finds four types of energy profiles for the Σ_g state, each defined by a different range of Z values. These are schematically illustrated in Fig. 4 for the Finkelstein-Horowitz approximation.

[5] See Ref. [6] for a detailed discussion of orbital distortion and its energetic consequences.

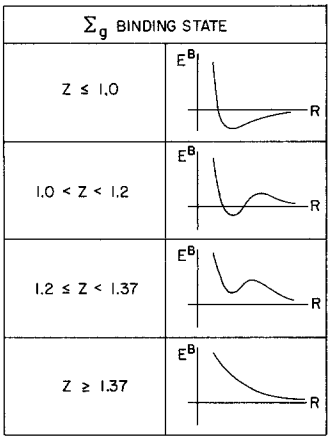

Fig. 4

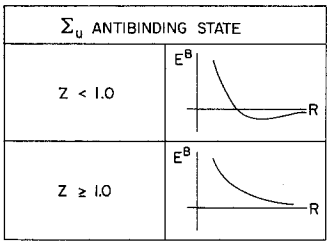

Fig. 5

Fig. 4. Energy curve profiles (schematic) for the Σ_g state

Fig. 5. Energy curve profiles (schematic) for the Σ_u state

For the Σ_u state, Fig. 3 shows that all curves possess a shallow minimum when $Z < 1.0$. The strongest bond occurs for $Z \sim 0.6$ for which $E^B \sim -0.02$ a.u. at $R_0 \sim 9.0$ a.u.[6]. If $Z \geqq 1.0$, the curves are everywhere repulsive. Fig. 5 schematically illustrates the two types of energy curves which occur for this state.

3. Origin of Potential Profiles

We now turn to the question why the energy curves depicted in Figs. 4 and 5 change their behaviour so significantly when Z is varied. Of particular interest is the origin of the "hump" in the Σ_g state and the slight binding character of the Σ_u state. The analysis of these phenomena becomes simple if one uses the approach advanced and elaborated in Ref. [6]. It leads to the conclusion that all aforementioned deviations from H_2^+ behaviour have their origin exclusively in long-range coulombic interactions. Thus, it follows that, in addition to the centrifugal potential associated with nuclear rotational motion and the mechanisms of predissociation, there exists a third reason for potential barriers, namely, long range coulombic repulsions. An interesting aspect of this mechanism is that it can introduce binding character into an "antibinding" state.

3.1. Conceptual Partitioning of the Energy for H_2^+

In the approximation of Eq. (11), the energy difference

$$E^B(R, 1) = E(H_2^+) - E(H)$$

can be partioned as follows[6]:

$$E^B(R, 1) = E^P(R, 1) + E^{QC}(R, 1) + E^I(R, 1) \tag{12}$$

[6] In Ref. [4], R_0 at the deepest minimum should be twice 4.6 a.u.

where

$$E^P(R,1) = \langle A| -\tfrac{1}{2}\nabla^2 - r_A^{-1}|A\rangle + \tfrac{1}{2}, \tag{13}$$

$$E^{QC}(R,1) = \langle A| -r_B^{-1}|A\rangle + R^{-1}, \tag{14}$$

$$E^I(R,1) = \{\pm 1/(1\pm S)\}\{\langle A| -\tfrac{1}{2}\nabla^2 - r_A^{-1} - r_B^{-1}|B\rangle - S\langle A| -\tfrac{1}{2}\nabla^2 - r_A^{-1} - r_B^{-1}|A\rangle\}. \tag{15}$$

These three components have the following physical interpretations:

a) E^P is the energy difference between a hydrogen *atom*, whose 1*s* wave function, A, is characterized by the orbital exponent ζ appropriate to the molecular wave function, and a hydrogen atom with $\zeta = 1.0$, i.e., in its ground state. E^P is called the *promotion energy*.

b) E^{QC} represents the *coulombic* interaction of a neutral hydrogen atom (with ζ equal to that of the molecular wave function) and a proton located at distance R. This is called the *quasiclassical energy*.

c) E^I is the product of the two factors enclosed in curly brackets in Eq. (15). (The $\pm$ signs in Eq. (15) apply to ψ_+ and ψ_-, respectively.) The first factor is the *bond order*. The second is Mulliken's *resonance* integral. It has been shown elsewhere [5, 6] that E^I describes the energetic consequences associated with *electron sharing*, that it contains the binding and antibinding effects arising from

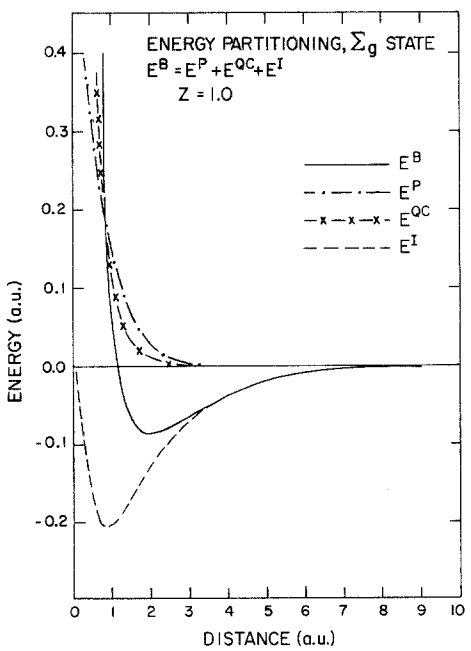

Fig. 6

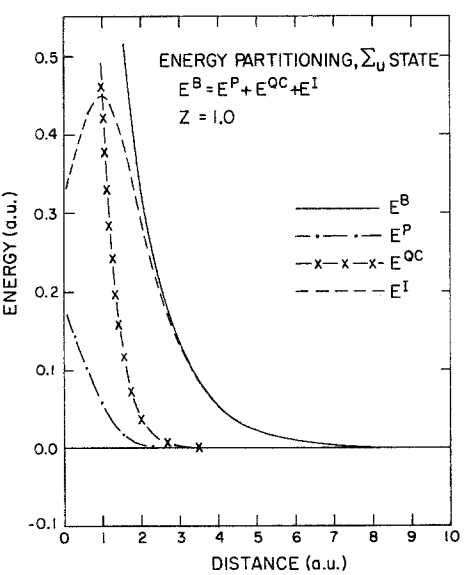

Fig. 7

Fig. 6. Energy partitioning for the Σ_g state of H_2^+ as functions of the internuclear distance (Finkelstein-Horowitz approximation)

Fig. 7. Energy partitioning for the Σ_u state of H_2^+ as functions of the internuclear distance (Finkelstein-Horowitz approximation)

the *overlap of atomic orbitals*, and that it can be interpreted as a wave *interference* of the atomic orbitals A and B. For this reason E^I is called the *interference energy*. It is negative for the Σ_g state and positive for the Σ_u state.

Figure 6 contains plots of $E^B(R, 1)$ and its three components for the Σ_g state as functions of the internuclear distance. These plots show that E^P, E^{QC} and E^I provide a convenient basis for a conceptual elucidation of the binding "process". It is seen, in agreement with general ideas, that the interference term E^I, which is associated with overlap, sharing, and resonance, yields the bond forming energy lowering. The promotion energy is a measure of the orbital contraction whose significance has been discussed in detail elsewhere [6]. It may be mentioned that for the exact wave function, the quasiclassical energy yields a slightly attractive curve due to orbital polarization [6]. It is apparent from Fig. 6 that the profile of the E^B curve is the result of a competition between E^I, E^P and E^{QC}, all of which decay exponentially with R.

The dominating role of E^I is further confirmed by an examination of the antibinding Σ_u state shown in Fig. 7. Whereas E^P and E^{QC} do not differ significantly from those of the Σ_g state, the E^I curve is now bond opposing throughout so that a repulsive E^B curve results.

3.2. *Analysis of (Z, Z) Energy Curves*

In analogy to the scaling relationships of Eqs. (3)–(4), the wave function for the (Z, Z) molecule-ion at distance R is obtained from the H_2^+ wave function by the scaling relationships

$$\psi(Z, R, r) = Z^{\frac{3}{2}}\psi(1, \bar{R}, \bar{r}), \tag{16}$$

$$\bar{R} = ZR, \bar{r} = Zr. \tag{17}$$

For the approximation of Eq. (11), one has therefore

$$\psi(Z, R, r) = [2(1 \pm S')]^{-\frac{1}{2}}[\mathrm{A}' \pm \mathrm{B}'] \tag{18}$$

where A′ and B′ are the appropriately modified 1*s* orbitals.

The energy of the (Z, Z) molecule-ion can be decomposed in a manner analogous to the partitioning of Eq. (12) for the H_2^+ molecule-ion:

$$E^B(R, Z) = E^P(R, Z) + E^{QC}(R, Z) + E^I(R, Z) \tag{19}$$

where now

$$E^P(R, Z) = \langle \mathrm{A}' | -\tfrac{1}{2}\nabla^2 - Zr_{\mathrm{A}}^{-1} | \mathrm{A}' \rangle + \tfrac{1}{2}Z^2, \tag{20a}$$

$$E^{QC}(R, Z) = \langle \mathrm{A}' | -Zr_{\mathrm{B}}^{-1} | \mathrm{A}' \rangle + Z^2 R^{-1}, \tag{21a}$$

$$\begin{aligned} E^I(R, Z) = \{\pm 1/(1 \pm S')\}\ \{&\langle \mathrm{A}' | -\tfrac{1}{2}\nabla^2 - Zr_{\mathrm{A}}^{-1} - Zr_{\mathrm{B}}^{-1} | \mathrm{B}' \rangle \\ &- S\langle \mathrm{A}' | -\tfrac{1}{2}\nabla^2 - Zr_{\mathrm{A}}^{-1} - Zr_{\mathrm{B}}^{-1} | \mathrm{A}' \rangle . \end{aligned} \tag{22a}$$

In view of Eqs. (5)–(7), (16)–(18), these terms can be obtained from the corresponding quantities for H_2^+:

$$E^P(R, Z) = Z^2 E^P(\bar{R}, 1), \tag{20b}$$

$$E^{QC}(R, Z) = Z^2 \left\{ E^{QC}(\bar{R}, 1) + \frac{Z-1}{\bar{R}} \right\}, \tag{21b}$$

$$E^I(R, Z) = Z^2 E^I(\bar{R}, 1). \tag{22b}$$

The application of these equations to an analysis of the (Z, Z) energy curves is carried out for four specific examples: $Z = 0.8$ and 1.3 for both the Σ_g and Σ_u states. The results are shown in Figs. 8, 9, 10, 11. In these graphs, the reduced energies $Z^{-2}E^B, Z^{-2}E^P, Z^{-2}E^{QC}, Z^{-2}E^I$ are plotted against the reduced internuclear distance, ZR.

Σ_g State

A comparison of Figs. 8 and 9 with Fig. 6 shows that the reduced promotion energies, $Z^{-2}E^P$, and the reduced interference energies, $Z^{-2}E^I$, are *identical* for all values of Z. The reduced quasiclassical energy is the only term which depends on Z. This is due to the fact that the long-range electron-nuclear attraction $(-Z \cdot 1/R)$ does not cancel the nuclear-nuclear repulsion Z^2/R, if $Z \neq 1$. The difference is contained in the $Z^2(Z-1)/\bar{R}$ term appearing in Eq. (21b). It shows that whereas the long range behaviour of E^{QC} is exponential for $Z = 1.0$ [see Eq. (14)], it has a long-range R^{-1} dependence for $Z \neq 1.0$: attractive for $Z < 1.0$, repulsive for $Z > 1.0$. Since E^P and E^I maintain their exponential dependence upon $\bar{R}$, the quasiclassical term becomes a major influence on the shape of the binding energy curve if $Z \neq 1.0$, whereas it is not for $Z = 1.0$. If $Z < 1.0$, it reinforces interference to enhance the reduced binding

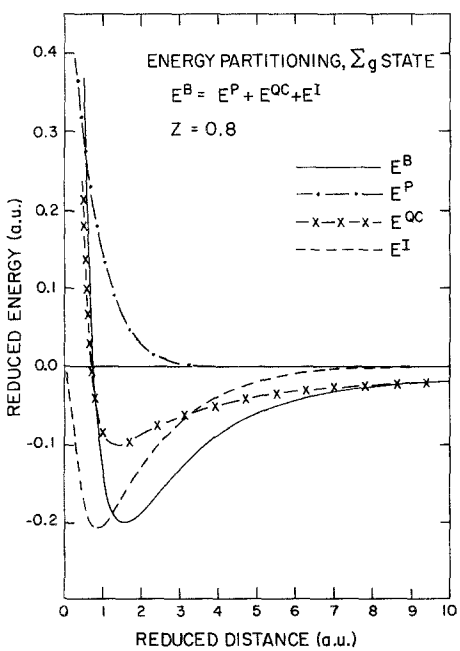

Fig. 8

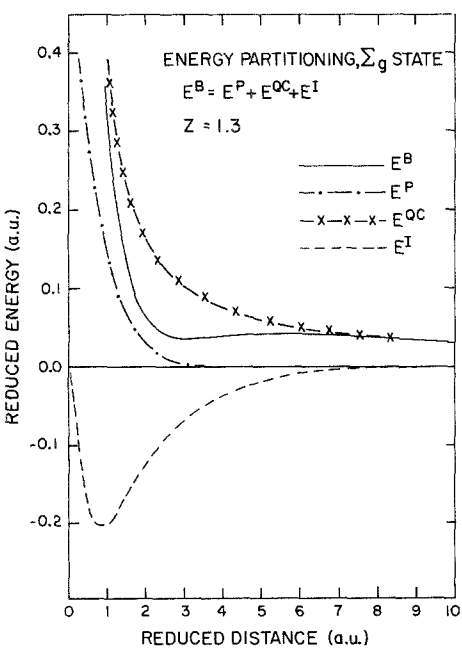

Fig. 9

Fig. 8. Energy partitioning for the Σ_g state for $Z = 0.8$ as functions of the internuclear distance (Finkelstein-Horowitz approximation)

Fig. 9. Energy partitioning for the Σ_g state for $Z = 1.3$ as functions of the internuclear distance (Finkelstein-Horowitz approximation)

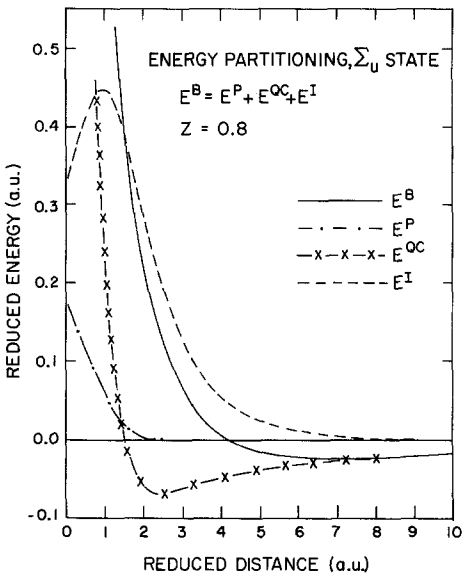

Fig. 10

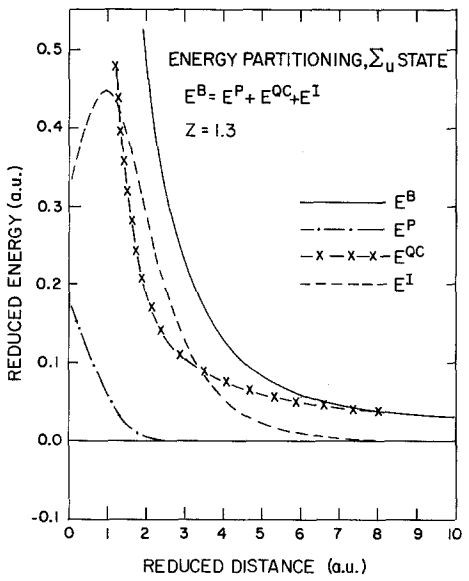

Fig. 11

Fig. 10. Energy partitioning for the Σ_u state for $Z = 0.8$ as functions of the internuclear distance (Finkelstein-Horowitz approximation)

Fig. 11. Energy partitioning for the Σ_u state for $Z = 1.3$ as functions of the internuclear distance (Finkelstein-Horowitz approximation)

energy. For $Z > 1.0$, it effectively opposes interference; it introduces the hump for $1.0 < Z < 1.2$; it raises the minimum above the dissociation limit for $1.2 \leqq Z < 1.37$; and it renders the curve everywhere repulsive for $Z \geqq 1.37$.

Σ_u *State*

Similar reasoning explains the behaviour of the Σ_u states shown in Figs. 10 and 11 for $Z = 0.8$, 1.3 as compared to that of H_2^+ shown in Fig. 7. As before, the reduced promotion and interference energies are identical for all values of Z, whereas the quasiclassical term acquires the same attractive or repulsive long-range behaviour as in the Σ_g state. In the Σ_u state, it successfully opposes the antibinding interference energy for $Z < 1.0$ to the extent that the Σ_u curve becomes slightly binding. For $Z \geqq 1.0$, it reinforces interference and thereby enhances the repulsive character of these curves.

4. Remarks

The present results were obtained by an analysis of the Finkelstein-Horowitz approximation. An analogous analysis can be made for the Guillemin-Zener function which represents a close approximation to the true solution for H_2^+. It is apparent that the same conclusions would be reached with only slight quantitative modification.

A similar type of analysis can also be applied to results for the two-electron case reported in Ref. [3]. However, a significant difference is found between the one- and two-electron cases. Whereas in the one-electron case the long-range behaviour of the quasiclassical energy is given by $Z(Z-1)/R$, the quasiclassical energy of the two-electron case has the long-range behaviour $(Z-1)^2/R$, which is repulsive for all $Z \neq 1.0$. Thus humps result for $Z < 1.0$ as well as for $Z > 1.0$.

Analogous characteristics can be expected in binding energy curves for more complex molecular-ions.

Acknowledgements. The author wishes to thank Professor Klaus Ruedenberg for several helpful suggestions and his critical reading of the manuscript. In addition the author is pleased to acknowledge the Ames Laboratory at Iowa State University for its hospitality during the Summer, 1969.

References

1. Pauling, L.: J. chem. Physics **1**, 56 (1933).
2. Fraga, S., Ransil, B. J.: J. chem. Physics **37**, 1112 (1962).
3. Feinberg, M. J., Haas, T. E.: Theoret. chim. Acta (Berl.) **7**, 290 (1967).
4. Cohen, M., McEachran, R. P.: Theoret. chim. Acta (Berl.) **12**, 87 (1968).
5. Ruedenberg, K.: Rev. mod. Physics **34**, 326 (1962).
   Edmiston, C., Ruedenberg, K.: J. physic. Chem. **68**, 1628 (1964).
   Layton, E. M., Jr., Ruedenberg, K.: J. physic. Chem. **68**, 1654 (1964).
   Rue, R. R., Ruedenberg, K.: J. physic. Chem. **68**, 1676 (1964).
   Moffat, J. H., Popkie, H. E.: Int. J. quant. Chemistry **2**, 565 (1968).
6. Feinberg, M. J., Ruedenberg, K., Mehler, E. L.: In: Advances in quantum chemistry, Vol. 5, ed. by P.-O. Löwdin, New York: Academic Press 1970.
7. Cohen, M., Dorrell, B. H., McEachran, R. P.: Theoret. chim. Acta (Berl.) **9**, 324 (1968).
8. Guillemin, V., Zener, C.: Proc. nat. Acad. Sci. USA **15**, 314 (1929).
9. Kim, S., Chang, T. Y., Hirschfelder, J. O.: J. chem. Physics **43**, 1092 (1965).
10. Löwdin, P.-O.: J. molecular Spectroscopy **3**, 46 (1959).
11. Finkelstein, B. N., Horowitz, G. E.: Z. Physik **48**, 118 (1928).

Prof. M. J. Feinberg
Department of Chemistry
Tufts University
Medford, Massachusetts 02155, USA